Rafidain Journal of Science

https://rsci.uomosul.edu.iq

Vol. 34, No. 4, pp. 90-101, 2025 (December)

Comprehensive Study for Ternary Alloys of Al-Cu-Sn and Al-Cu-Zn with Testing Compression and Corrosion

Raiq R.O. Al-Nima **Mahmood A.H. Al-jiboori**

Department of Physics / College of Science / University of Mosul/ Iraq

p-ISSN: 1608-9391
e -ISSN: 2664-2786

Article information

Received: 23/2/2025
Revised: 1/5/2025
Accepted: 11/5/2025

DOI: 10.33899/rjs.2025.190521

corresponding author:
Raiq R.O. Al-Nima
raiq.scp83@student.uomosul.edu.iq
Mahmood A.H. Al-jiboori
dr.mahmood@uomosul.edu.iq

ABSTRACT

Cast ternary alloys are significantly considered to be studied. For example, aluminum (Al), copper (Cu), and tin (Sn) construct the ternary alloy of Al-Cu-Sn. Another example is the aluminum (Al), copper (Cu), and zinc (Zn), which construct the ternary alloy of Al-Cu-Zn. Each one of them is established under the condition of very high temperatures. Their elements are collected, adjusted, and chopped. So, the ternary cast alloys are manufactured. Then, important mechanical tests of compression and corrosion are carried out and compared. The compression test is conducted on each alloy of Al-Cu-Sn and Al-Cu-Zn. It can be yielded that the highest compression value is recorded as Zn=0% and Sn=0%, but the lowest compression value is reported as Zn=10% and Sn=10%. On the other hand, the influence of corrosion tests on both alloys is found to be insignificant. Key findings of compression results, which are tied to Zn/Sn concentrations, are that when Zn=0% and Sn=0%, brittle status has been confirmed, while when Zn=10% and Sn=10%, ductile status has been approved.

Keywords: Ternary alloys, compression test, corrosion test.

INTRODUCTION

Combining Al, Cu, Sn, Al, Cu, and Zn can provide such intriguing cast alloys (Kotadia *et al*., 2009; Michalik and Chmiela, 2015; Klopotov *et al*., 2016; Villalta-Cerdas and McCleary, 2019). To illustrate, their ternary cast alloys may provide such mechanical properties of hardness, compression, sheer stress, fatigue resistance and corrosion (Ezenwelu *et al*., 2024; Ali *et al*., 2024; Michalik and Tomaszewska, 2016; Ferdian *et al*., 2017; Wang *et al*., 2019). They are used in some important manufactures, such as industrial, automotive parts, bodies of buses, beverage cans and biological activity (Abdljabar and Saeed, 2024; Kim *et al*., 2008; Khan *et al*., 2023; Osten *et al*., 2020; Shekha and Mohammedamin, 2024).

Different studies were presented in the literature for utilizing the Al-Cu-Sn and Al-Cu-Zn alloys, such as

In 2012, Yan *et al*. observed the Al–Cu–Sn immiscible alloy. Ultrasonic levitation conditions were used. Alloy structure evolution and phase separation were both discovered. Theoretical assessment provided that the morphology transition was essentially based on the surface tension and density variances. Specifically, between the liquid phases of Sn-rich and Al-rich (Yan *et al*., 2012). In 2015, Lee and Ahn worked on the influence of sintering temperature and compaction pressure. The Al-Cu-Zn alloy behavior was comprehensively discussed for sintering of the liquid phase. The sintering operation was implemented at different temperature conditions. The nitrogen (N_2) gas atmosphere was also applied with the various temperatures (Lee and Ahn, 2015). In 2016, Zhang *et al*. explained the influences of normal load and sliding velocity. Tribological behavior was concentrated for the aged alloy of Al-Sn-Cu. Peak-aged (PA), under-aged (UA), and over-aged (OA) alloys were explored and compared. The results yielded that the PA obtained a better tribological behavior than the others. This might be because of a better hardness and the matching of optimized strength-ductility (Zhang *et al*., 2016). In 2018, Rafla *et al*. described galvanic corrosion operando evaluation. Stainless steel fasteners and Al-Zn-Mg-Cu alloys were explored. X-ray tomography was utilized. The damage morphology was measured with X-ray tomography. It compared accelerated exposures of laboratory-produced data in addition to field data. It was discovered to possess similar morphologies (Rafla *et al*., 2018). In 2021, Ćorić and Žmak concentrated on the effect of ausforming treatment. Super elasticity for the shape memory alloy of Cu-Zn-Al was assessed. Seismic energy dissipaters were taken into account. It was revealed that attaining an optimal fusion was possible for improved transformation behavior and adequate strength of the Cu-Zn-Al alloy. This was by employing the ausforming treatment (Ćorić and Žmak, 2021). In the same year, Akopyan *et al*. illustrated the hardening response of precipitation and structure. Manufactured and cast Al-Cu-Sn alloy was utilized. In this study, the addition of trace amounts of Sn was found to catalyze precipitation hardening. Furthermore, the peak hardness is around 20% more than what could be achieved for the Sn-free alloy. In addition, the Sn-free alloy was accomplished much faster. The limitation of Sn trace addition was related to the growth of the Cu-rich phase (Akopyan *et al*., 2021). In 2023, Edoziuno *et al*. explained grain size organization and morphological development. Addressing treated and as-cast Cu-Zn-Al alloy were utilized. Enhanced shape memory alloys of ternary Cu-20Zn-6Al were considered for exploitation in a crucible furnace of oil-fired casting. The generated alloys might be utilized in applications of structural vibration damping due to the anticipated development in shape memory and mechanical qualities as an outcome of the homogeneity of grains and dramatic purification investigated after addressing treatment (Edoziuno *et al*., 2023).

It can be investigated from this literature that many studies were provided for the Al-Cu-Sn and for the Al-Cu-Zn alloys. Nevertheless, there are still more explorations required. In this study, manufacturing ternary alloys of Al-Cu-Zn and Al-Cu-Sn is considered with the application of significant evaluations and comparisons of mechanical properties. Hence, the novelty of comparing Al-Cu-Sn and Al-Cu-Zn is considered, where each one of these ternary alloys has such significant characteristics. For example, it is estimated that Al-Cu-Zn will be more ductile than Al-Cu-Sn;

however, this can be approved in this study. More comparisons of characteristics can also be investigated.

The aim of this paper is to establish and evaluate Al-Cu-Sn and Al-Cu-Zn cast alloys. The contributions here are revealed as follows:

- Manufacturing Al-Cu-Sn cast alloys.
- Manufacturing Al-Cu-Zn cast alloys.
- Applying different tests of mechanical properties, such as compression and corrosion, to the cast alloys.
- Providing extensive comparisons of results between all manufactured cast alloys.

The sections of this paper are distributed as follows: The introduction is provided in section 1, prior studies are reviewed in section 2, the methodology or theoretical part is explained in section 3, practical results are discussed in section 4, and the conclusion is revealed in section 5.

THEORETICAL PART

As mentioned, here the ternary alloys of Al-Cu-Sn and Al-Cu-Zn have been focused on. To justify the selection of Al-Cu-Sn and Al-Cu-Zn is that their concentrations are significant. That is, the pure Al, Cu, Sn, and Zn have been purchased as Al saturation of 98%, Cu saturation of 99%, Zn saturation of 99%, and Sn saturation of 99%. Moreover, changing percentages of these concentrations (weights) are applied for each cast alloy as $Al_{90}Cu_{10-x}Sn_x$ and $Al_{90}Cu_{10-x}Zn_x$, where x=0,2,4,6,8,10. Fig. (1) demonstrates the diagrams of triple phases for Al-Cu-Sn and Al-Cu-Zn, respectively.

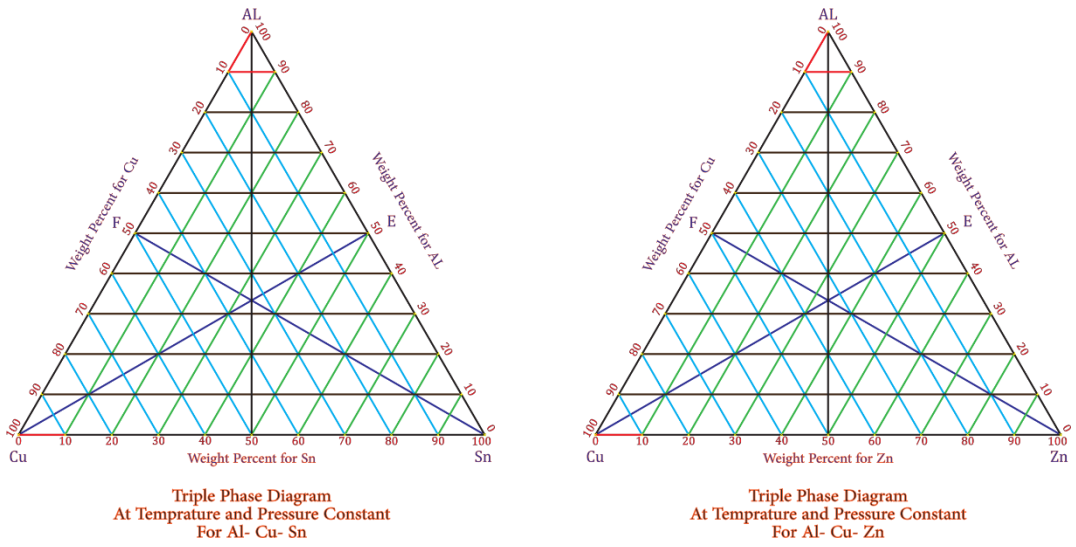

(a) **(b)**

Fig. 1: Diagrams of triple phases (a) the triple phase diagram for Al-Cu-Sn and (b) the triple phase diagram for Al-Cu-Zn.

In this paper, extensive processes are employed, each of which has a reasonable theory. They consist of multiple stages. First stage: Acquiring material elements of Al, Cu, Sn, and Zn. Second stage: Preparing the pure Al, Cu, and Sn for Al-Cu-Sn cast alloys; similarly, preparing the Al, Cu, and Zn for Al-Cu-Zn cast alloys. Third stage: Changing percentages of weights are applied during the cast alloy manufacture. Fourth stage: Manufacturing multiple cast alloys for each of the two groups, Al-Cu-Sn and Al-Cu-Zn. Fifth stage, chopping the cast alloys into regular pieces. Sixth stage, rubbing each cast alloy while taking into account multiple measurements of cutting ratio (R). Seventh stage: Mechanical tests of corrosion and compression are considered for evaluation. In the final stage, recording outcomes are analyzed and benchmarked. Fig. (2) shows the block diagram of the considered procedure.

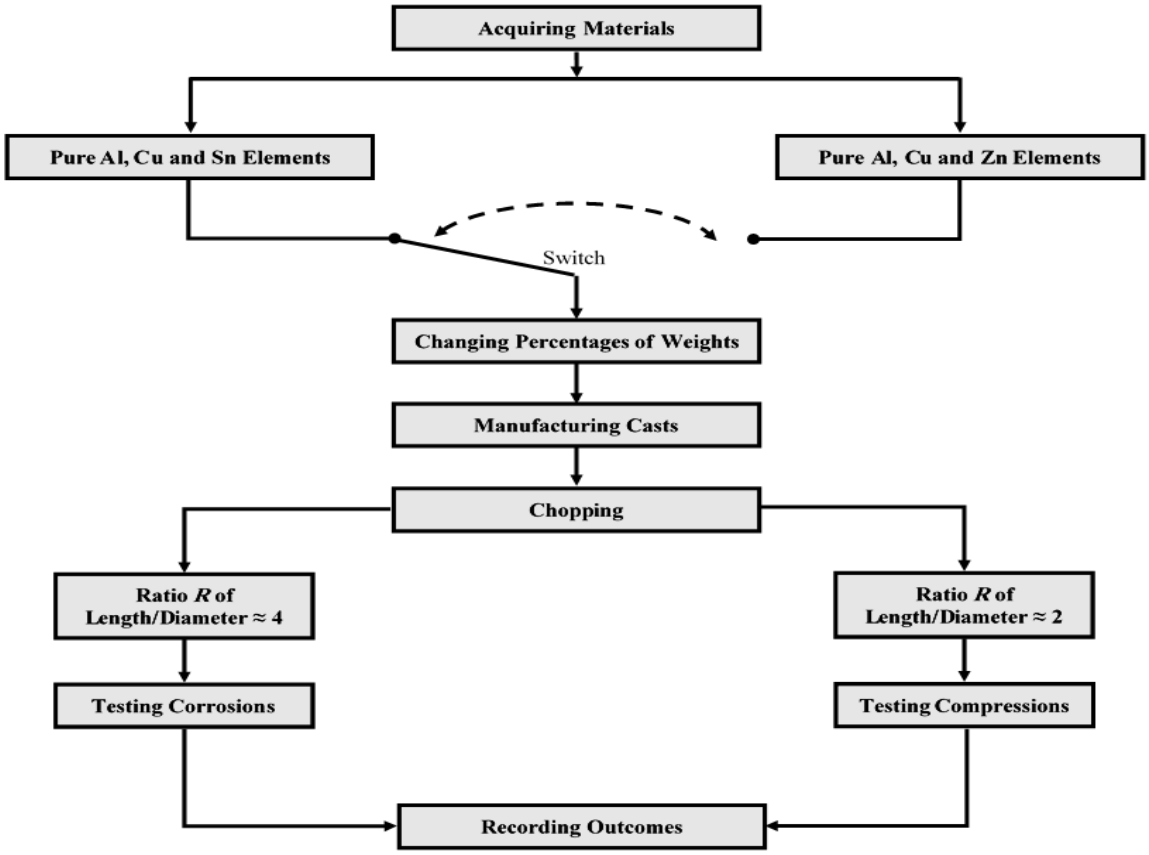

Fig. 2: Block diagram of the considered procedure.

With more illustration, acquiring material elements includes looking for and purchasing pure Al, Cu, Sn, and Zn. Then, the collected elements are grouped into Al, Cu, and Sn as a group 1, and Al, Cu, and Zn as a group 2. Each group is used to prepare its cast alloys of Al-Cu-Sn and Al-Cu-Zn. Fundamentally, the saturations of pure elements Al, Cu, Sn, and Zn were first acquired as 98%, 99%, 99%, and 99%, respectively. Henceforth, changing percentages of weights (with considering Al is constant) are applied for the Cu and Sn and applied for the Cu and Zn (Al-Nima and Al-jiboori, 2024). (Table 1) shows the considered ratios and weights for the Al-Cu-Sn. Whereas, (Table 2) provides the utilized ratios and weights for the Al-Cu-Zn.

Table 1: The utilized ratios and weights for the pure Al, Cu and Sn.

Index	Al (%)	Cu (%)	Sn (%)	Al (gm)	Cu (gm)	Sn (gm)
B1	90	10	0	18	2	0
B2	90	8	2	18	1.6	0.4
B3	90	6	4	18	1.2	0.8
B4	90	4	6	18	0.8	1.2
B5	90	2	8	18	0.4	1.6
B6	90	0	10	18	0	2

Table 2: The utilized ratios and weights for the pure Al, Cu and Zn.

Index	Al (%)	Cu (%)	Zn (%)	Al (gm)	Cu (gm)	Zn (gm)
A1	90	10	0	18	2	0
A2	90	8	2	18	1.6	0.4
A3	90	6	4	18	1.2	0.8
A4	90	4	6	18	0.8	1.2
A5	90	2	8	18	0.4	1.6
A6	90	0	10	18	0	2

Furthermore, the cast alloys are manufactured by providing a high temperature in order to melt and mix the Al-Cu-Sn and Al-Cu-Zn. That is, the Cu was melted in a gas furnace under the high temperature. Subsequently, the Al was included and merged with the Cu inside the gas furnace. Consequently, the Sn was also added and mixed with the Al-Cu in the gas furnace too. Similarly, more Cu was melted also in the same gas furnace and under a high temperature. After that, the Al was provided and combined with the Cu inside the same gas furnace. Then, the Zn was included and merged with the Al-Cu in the gas furnace too. Fig. (3a) shows the gas furnace that has been used for manufacturing the cast alloys. So, both groups of cast alloys are melted and carefully mixed together until homogenous, at which point the Al-Cu-Sn and Al-Cu-Zn are finally established. Such manufacturing has been repeated many times, where multiple ternary alloys of Al-Cu-Sn and Al-Cu-Zn are obtained.

Consequently, chopping the cast alloys is carried out after their high temperatures have vanished. A total of 12 pieces are equally chopped by considering regular measurements. Then, the cutting ratio (R) is rubbing each one of the cast alloys, where R is denoted as the ratio of length to diameter; it is also considered as the standard mechanical testing protocol. In this paper, R is taken as R≈2 and R≈4. Principally, R≈2 measurements of testing compressions and R≈4 measurements of testing corrosions. This is because R≈2 can be considered as a standard cutting ratio for the testing compression, while the reason for R≈4 is appropriate for discovering the amount of corrosion in its testing, and all components are inside the alloys.

With more illustration, testing compression is utilized based on the following equations:

$$\sigma = \frac{F}{A} \quad \ldots\ldots\ldots\ldots\ldots\ldots (1)$$

Where: σ is the compression measurement with the unit newton divided by square meters (N/m^2), F Is the force with the unit newton (N) and A is the area with the unit square meters (m^2), which is also considered as:

$$A = \pi\, r^2 \quad \ldots\ldots\ldots\ldots\ldots\ldots (2)$$

Where: π represents the known pi constant and r represents the radius of a circle sample (Callister and Rethwisch, 2007; Fragassa *et al*., 2016; Scari *et al*., 2014; Strauss *et al*., 2005).

Additionally, the strain and Young's modulus are calculated. Strain is expressed as follows:

$$\epsilon = \frac{l_i - l_0}{l_0} = \frac{-\Delta l}{l_0} \ldots\ldots\ldots\ldots (3)$$

Where: ϵ represents the strain (without unit), l_i represents the far end length of the considered sample, l_0 represents the prior end length of the considered sample, Δl represents the difference in length, and the negative sign represents the compression (Callister and Rethwisch, 2007; G *et al*., 2012; Fragassa *et al*., 2016; Scari *et al*., 2014).

Young's measurement by (N/m^2) unit can be computed according to the following equation:

$$Y = \frac{\sigma}{\epsilon} = \frac{F\, l_0}{A\, \Delta l} \ldots\ldots\ldots (4)$$

Where: Y is the Young's modulus (Callister and Rethwisch, 2007; Fragassa *et al*., 2016).

Testing corrosion is employed for R≈4. A total of 12 pieces of cast alloys are manufactured for Al-Cu-Sn and Al-Cu-Zn, divided as 6 samples for Al-Cu-Sn and the remaining 6 samples for Al-Cu-Zn. Each sample is weighed before putting it inside the electric furnace; such weight is called the standard weight. All samples are being inside the electric furnace for a long time with high temperature (nearly 5 hours at 400°C) (Yang *et al*., 2019). After taking the samples outside the electric furnace, each sample is weighed again after its high temperature vanishes. Such processes of putting the samples inside the electric furnace, taking them out, waiting for their high temperatures to vanish,

and measuring the weights are repeated again for 35 times with 175 hours (actually around three months). Fig. (3b) shows the employed electric furnace for corrosion testing.

(a) (b)

Fig. 3: The used furnaces (a) the gas furnace for manufacturing the cast alloys (Al-Nima, 2021) and (b) the employed electric furnace for corrosions testing (Al-Nima, 2021; Ikhdhayyir and Hammoud, 2022).

Hence, the differences in weights are calculated as the measured weight after the furnace minus the standard weight divided by the surface area of a sample.

Finally, the outcomes of mechanical measurements are recorded, analyzed, and compared for the manufactured cast alloys.

PRACTICAL PART WITH DISCUSSIONS

First of all, multiple cast alloys of pure Al-Cu-Sn and pure Al-Cu-Zn have been manufactured. For any alloy, a pure element, Cu, was first put in a pot, and a very high temperature was applied (greater than 1080°C) by using a gas furnace, so the pure Cu element was melted. Secondly, the Al element has been added to the same pot of melted Cu. They all put in the same gas furnace again, where Al has been mixed with Cu by using a rod of carbon (C), and they gradually melted to get a homogenous liquid. Thirdly, the Sn element has been included in the melted Al-Cu inside the same pot and quickly mixed by using the rod of C too. The reason for quickly mixing here is that Sn melts faster than other elements; it has a low melting point (231.9°C). Fourthly, the mixed liquid of Al-Cu-Sn has been spilled into a mold of steel and concrete, which is specifically designed for forming the alloys. Similar processes have been repeated again, but this time for the Al-Cu-Zn, taking into account that Zn also melts faster than other elements; it has a low melting point (231.9°C). The preparation temperatures for manufacturing the considered alloys are between 1080°C and 231.9°C. Sample dimensions for each cast alloy in the case of compression testing are diameter≈1.1cm and height≈2.2cm. Sample dimensions for each cast alloy in the case of corrosion testing are diameter≈1.1cm and height≈4.4cm. Moreover, all processes have been repeated many times for the 24 samples of the Al-Cu-Sn and Al-Cu-Zn. They basically divided into two sets: 12 samples with compression testing and 12 samples with corrosion testing.

The considered ratios and weights ( ) for the pure Al-Cu-Sn are provided in Table (1). Whereas, the considered ratios and weights for the pure Al-Cu-Zn are provided in Table (2).

The established cast alloys for the two groups of pure Al-Cu-Sn and pure Al-Cu-Zn have been chopped with R≈2 for compression testing and R≈4 for corrosion testing

Compression testing

The compression has been taken into account for all the manufactured cast alloys. More exclusively, the strain, fraction stress and Young's modulus have been assessed with respectively the ϵ, σ and Y parameters. For evaluating the compression, a press device of type (STENHØJ A/S, DK 7150 BARRIT DENMARK) with σ = 40 tons have been used. In addition, equations (1), (2), (3),

and (4) have been calculated. Tables (3) and (4) provide the measurements and details of the pure Al-Cu-Sn and pure Al-Cu-Zn cast alloys, respectively.

Table 3: The considered ratios and weights for the pure Al-Cu-Sn.

Index	Sn (wt%)	ϵ (-)	σ in Mpa	Y in Gpa (-)
B1	0	0.2067308	455.98935	2.2057159
B2	2	0.2631579	273.59361	1.0396557
B3	4	0.28	182.39574	0.6514134
B4	6	0.2941176	136.79681	0.4651091
B5	8	0.3368421	91.19787	0.2707437
B6	10	0.3608247	68.398403	0.1895613

Table 4: The considered ratios and weights for the pure Al-Cu-Zn.

Index	Zn (wt%)	ϵ (-)	σ in Mpa	Y in Gpa (-)
A1	0	0.1791045	455.98935	2.5459405
A2	2	0.1904762	182.39574	0.9575776
A3	4	0.21	136.79681	0.6514134
A4	6	0.2242152	91.19787	0.4067425
A5	8	0.2682927	68.398403	0.2549395
A6	10	0.2985075	45.598935	0.1527564

It can be noticed from (Table 3) that the evaluated ratios of Al, Cu, and Sn have been grouped for obtained performances. Six points have been determined in this study. These are for the Al ratio of 90% and Cu+Sn ratios between 10% and 0%, decreasingly. The highest strain value is recorded when the Al, Cu, and Sn ratios are 90%, 0%, and 10%, respectively. The lowest strain value is benchmarked when the Al, Cu, and Sn ratios are 90%, 10%, and 0%, respectively.

Similarly, it can be observed from (Table 4) that the evaluated ratios of Al, Cu, and Zn have been grouped for obtained performances. Six points have also been determined here. These are for the Al ratio of 90% and Cu+Zn ratios between 10% and 0%, decreasingly. The highest strain value is recorded when the Al, Cu, and Zn ratios are 90%, 0%, and 10%, respectively. The lowest strain value is benchmarked when the Al, Cu, and Zn ratios are 90%, 10%, and 0%, respectively.

These performances depict curves here because of adding an effective element of Sn or Zn. Such an influential element can substantially affect the compressing calculations even with a little ratio. Fig. (4a) demonstrates the relationships between the fraction stress measurements and strain ratios for the cast alloys of pure Al-Cu-Sn. Fig. (4b) demonstrates the fraction stress measurements and strain ratios for the cast alloys of pure Al-Cu-Zn.

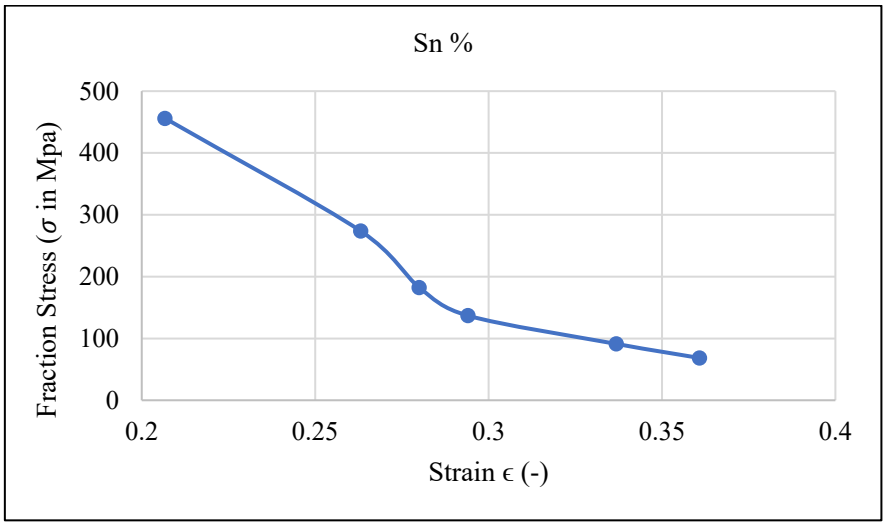

(a)

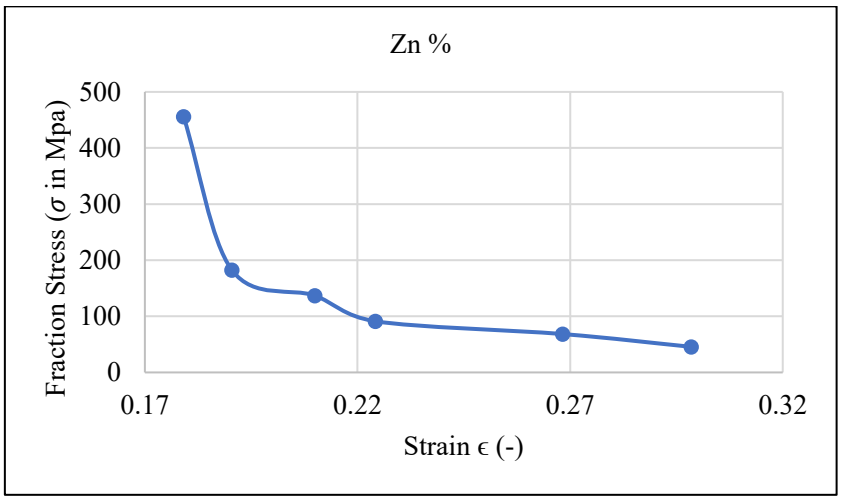

(b)

Fig. 4: Relationships between the fraction stress measurements and strain ratios (a) for the pure Al-Cu-Sn cast alloys and (b) for the pure Al-Cu-Zn cast alloys.

The main difference between the performances of the pure Al-Cu-Sn group and the pure Al-Cu-Zn group is that the ϵ, σ and Y evaluations have different values. This is reasonable, as the performances of the pure Al-Cu-Sn group and pure Al-Cu-Zn group are affected by the different properties of their additional elements (Sn or Zn).

For explaining the mechanistic roles of Sn and Zn in compression outcomes, it is approved that Al-Cu-Sn is less ductile than Al-Cu-Zn. Such outcomes are consistent with what has been expected. On the other hand, the cast alloys without adding Sn or Zn have obtained higher compression outcomes than the cast alloys with any of these elements added. This yields the existence effectiveness of Sn or Zn to the cast alloys.

Corrosion testing

Due to the fact that the beginning of corrosion is oxidation, where material is corroded and oxidized to get stability through interacting with the environment. Essentially, active materials interact with the environment to form compounds.

The process of reacting between an element material and oxygen forms an oxidation layer on the element. This is a self-defense process carried out by the material to protect itself from corrosion. Therefore, there are some significant points that can be highlighted here:

- Highly adhesive oxidation layer causes increasing weight gain.
- Non-adherent oxidation layer can be peeled off, which means losing weight.
- Losing weight also occurs in the absence of oxidative stress due to the formation of volatile oxides.

However, it is noted in this study that the color, dimensions, and weights of the alloys have not been changed (or have been very slightly changed) for all samples of pure Al-Cu-Sn and pure Al-Cu-Zn groups. Fig. (5) demonstrates the relationships between the differences in weights and time for the pure Al-Cu-Sn cast alloys and for the pure Al-Cu-Zn cast alloys.

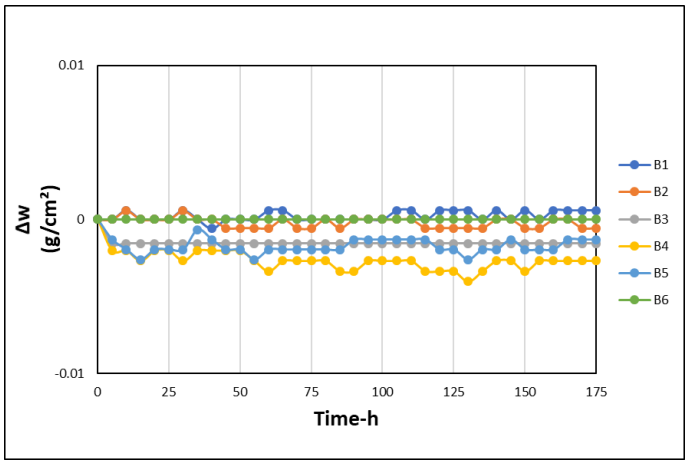

(a)

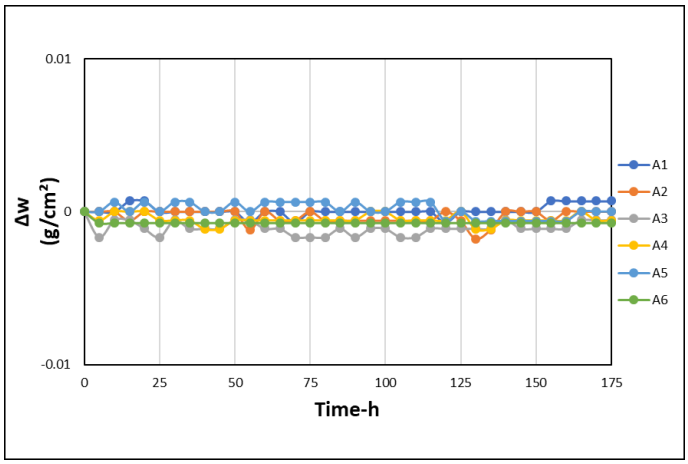

(b)

Fig. 5: Relationships between the differences in weights and time (a) for the pure Al-Cu-Sn cast alloys and (b) for the pure Al-Cu-Zn cast alloys.

The outcomes in Fig. (5a: B1, B2) and Fig. (5b: A1, A2, A4, A5) illustrate the mechanism of oxidation. No significant changes in weights have been observed throughout the period of cyclic oxidation. So, conservative oxide crusts of (Al_2O_3) and (Al_2Cu) are formed. Such outcomes are consistent with the formation of resistant phases of (Al and Cu) where good mechanical specifications are provided. Moreover, the performances for the mechanism of oxidation in Fig. (5a: B4, B5) and Fig. (5b: A3) show that the weights of samples have very slight changes at the start of the thermal cycles. Noticeably, the shells of oxide do not fall off from all samples. This indicates that the forming of (Al_2O_3) oxide shells after the third cycle and a long thermal cycle is for protection. The samples have stability and decreasing weights, which signifies the formation of volatile oxides. In addition, the results in Fig. (5a: B3, B6) and Fig. (5b: A6) demonstrate for the mechanism of oxidation that their samples have very high stability over a long thermal cycle. This refers to the formed (Al_2O_3) that adds protected oxide shells with high adhesion. The formed shells are to protect the samples from the external environment through periods of thermal cycles. Finally, all samples' shapes are observed to have no change in color or dimensions.

Essentially, Al cast alloys already have the characteristic of corrosion resistance. So, adding the element of Sn or Zn, corrosion resistance has been further increased. This is reasonable, as that is why the differences in corrosion results are found to be insignificant. Furthermore, corrosion rates have also shown insignificant values due to the same reason. Generally, corrosion results may lead to similar outcomes.

In literature studies, there is work on the Al-Cu-Sn and on Al-Cu-Zn alloys. Nonetheless, more discovering is still required. So, this study has considered manufacturing the ternary alloys of Al-Cu-Sn and Al-Cu-Zn. Then, significant evaluations and comparisons are applied for mechanical properties. The considered cast alloys can be applied in critical industries such as building ships and airplanes.

CONCLUSIONS

This paper presented the manufacturing of ternary alloys of Al-Cu-Sn and Al-Cu-Zn. In addition to applying compression and corrosion tests. The work here was designed as follows: Collecting the Al, Cu, Sn, and Zn materials; grouping them into pure Al-Cu-Sn and pure Al-Cu-Zn; changing percentages of mixed Cu, Sn, or Zn weights; establishing multiple ternary cast alloys of pure Al-Cu-Sn and pure Al-Cu-Zn; chopping the cast alloys; applying effective measurements (the Young's modulus, fraction stress, and strain); and extensively discussing and comparing the main outcomes.

Multiple results have been obtained in this study. The measured ϵ, σ and Y values for the cast alloys of pure Al-Cu-Sn and pure Al-Cu-Zn appeared to be gradually decreasing. Furthermore, the pure Al-Cu-Sn cast alloys were more ductile than pure Al-Cu-Zn cast alloys. This is due to the effect of adding the embedded elements of Sn or Zn. Also, it was observed that the pure Al-Cu cast alloys for the two groups had higher fraction stress than pure Al-Sn and Al-Zn cast alloys. This is due to the effect of with or without the existing Sn or Zn elements.

For the corrosion tests, it could be yielded that there were no changes in dimensions, weights, and color for the cast alloys of pure Al-Cu-Sn and pure Al-Cu-Zn. For all outcomes, it could be concluded that there were noteworthy influences of involving an additional element (Sn or Zn) in the cast alloys according to their properties.

Practical implications of Al-Cu-Sn and Al-Cu-Zn cast alloys are that they may significantly improve various fields of industry, agriculture, and commerce. For industrial relevance, a further goal or aim can be represented by exploiting the considered cast alloys in critical industries such as building airplanes and ships.

For future work, characterization can be considered with energy dispersive X-Ray (EDX), X-Ray diffraction (XRD), therapeutic goods administration (TGA), differential scanning calorimetry (DSC), scanning electron microscopy (SEM), and transmission electron microscopy (TEM) to validate the results.

REFERENCES

Abdljabar, R.R.; Saeed, F.T. (2024). Synthesis and characterization of Mn (II), Co (II), Ni (II), Cu (II) and Zn (II) complexes with heterocyclic ligands and evaluation of its biological activity. *Raf. J. Sci.*, **33**(4), 56-68. DOI:10.33899/rjs.2024.185384

Akopyan, T.K.; Shurkin, P.K.; Letyagin, N.V.; Milovich, F.O.; Fortuna, A.S.; Koshmin, A.N. (2021). Structure and precipitation hardening response in a cast and wrought Al-Cu-Sn Alloy. *Mat. Lett.*, **300**, 130090. DOI:10.1016/j.matlet.2021.130090

Ali, F.N.M.; Al-Fulayih, R.Z.A.; Salman, Y.A.K. (2024). Effect of chromium plating of AISI 321 alloy at 1000°C on fatigue resistance article information. *Raf. J. Sci.*, **33**(4), 118-125. DOI:10.33899/rjs.2024.185389

Al-Nima, R.R.O. (2021). Manufacturing Al-Cu and Al-Cu-Mg alloys with studying some of their mechanical properties. Master thesis, Department of Physics, University of Mosul, Iraq.

Al-Nima, R.R.O.; Al-jiboori, M.A.H. (2024). Manufacturing ternary alloys of Al-Cu-Zn and Al-Cu-Sn with hardness and tensile strength testing. *Sixth Inter. Sci. Confer. Sci. Tech.*, Iraq-Dauhok, 23-27.

Callister, W.D.; Rethwisch, D.G. (2007). "Fundamentals of Materials Science and Engineering, An Integrated Approach". 3rd ed., 2008 John Wiley & Sons, Inc.

Ćorić, D.; Žmak, I. (2021). Influence of ausforming treatment on super elasticity of Cu-Zn-Al shape memory alloy for seismic energy dissipaters. *Build*., **11**(1), 22. DOI:10.3390/buildings11010022

Edoziuno, F.O.; Nwaeju, C.C.; Nnuka, E.E. (2023). Morphological evolution and grain size distribution of As-cast and solution treated Cu-Zn-Al alloy. *UNIZIK J. Eng. App. Sci.*, **1**(1), 23-30.

Ezenwelu, C.O.; Okeke, C.M.; Udemezue, O.I.; Ngwu, O.R.; Ogana, J.; Oparaji, E.H. (2024). Assessment of differential sheer stress indices in agricultural soil receiving cafeteria effluent. *Raf. J. Sci.*, **33**(1), 42-48. DOI:10.33899/rjs.2024.182825

Ferdian, D.; Pratesa, Y.; Togina, I.; Adelia, I. (2017). Development of Al-Zn-Cu Alloy for low voltage aluminum sacrificial anode. *Proc. Eng.*, **184**, 418-22. DOI:10.1016/j.proeng.2017.04.112

Fragassa, C.; Radovic, N.; Pavlovic, A.; Minak, G. (2016). Comparison of mechanical properties in compacted and spheroidal graphite irons. *Trib. Ind.*, **38**(1), 45-56. DOI:11585/534239

G, D.S.; J, O.; N, E.I.D. (2012). The effect of sand casting process parameters on mechanical properties of aluminium casting. *Inter. J. Metall. Mat. Sci. Eng.*, **2**(3), 32-41.

Ikhdhayyir, T.M.; Hammoud, M.A. (2022). Efficiency study of AISI-304L stainless steel alloy coated with the presence of the thermal barrier at high temperatures. *Raf. J. Sci.*, **31**(3), 18-29. DOI:10.33899/rjs.2022.175401

Khan, A.M.; Xu, C.; Hamza, M.; Afifi, A.M.; Qaisrani, N.A.; Sun, H.; Wang, B.; Khan, W.Q.; Yasin, G.; Liao, W-B. (2023). Enhanced tensile strength in an Al–Zn–Mg–Cu alloy via engineering the precipitates along the grain boundaries. *J. Mat. Res. Tech*., **22**, 696-705. DOI:10.1016/j.jmrt.2022.11.155

Kim, S.-J.; Kim, K.-S.; Kim, S.-S.; Kang, C.-Y.; Suganuma, K. (2008). Characteristics of Zn-Al-Cu alloys for high temperature solder application. *Mat. Trans*., **49**(7), 1531-36. DOI:10.2320/matertrans.MF200809

Klopotov, A.; Ivanov, Y.; Vlasov, V.; Dedov, N.; Loskutov, O.; (2016). "Phase Transformations in the System Cu-Zn-Al under Conditions Far from Equilibrium". In AIP Conference Proceedings, Vol. 1698, AIP Publishing.

Kotadia, H.R.; Doernberg, E.; Patel, J.B.; Fan, Z.; Schmid-Fetzer, R. (2009). Solidification of Al-Sn-Cu based immiscible alloys under intense shearing. *Metallur. Mat. Trans. A*, **40**, 2202-11. DOI:10.1007/s11661-009-9918-x

Lee, S.H.; Ahn. B. (2015). Effect of compaction pressure and sintering temperature on the liquid phase sintering behavior of Al-Cu-Zn alloy. *Arc. Metallur. Mat*., **60**(2B), 1485-89. DOI:10.1515/amm-2015-0158

Michalik, R.; Tomaszewska, A. (2016). An influence of ageing on the structure, corrosion resistance and hardness of high aluminum ZnAl40Cu3 alloy. *Arc. Metallur. Mat.*, **61**(1), 289-94. DOI:10.1515/amm-2016-0055

Michalik, R.; Chmiela, B. (2015). Study on nanohardness of phases occurring in ZnAl22Cu3 and ZnAl40Cu3 alloys. *Arc. Metallur. Mat*., **60**(2A), 621-26. DOI:10.1515/amm-2015-0182

Osten, J.; Milkereit, B.; Reich, M.; Yang, B.; Springer, A.; Nowak, K.; Kessler, O. (2020). Development of precipitation hardening parameters for high strength alloy AA 7068. *Mat*., **13**(4). DOI:10.3390/ma13040918

Rafla, V.N.; King, A.D.; Glanvill, S.; Davenport, A.; Scully, J.R. (2018). Operando assessment of galvanic corrosion between Al-Zn-Mg-Cu alloy and a stainless steel fastener using x-ray tomography. *Corro.*, **74**(1), 5-23. DOI:10.5006/2561

Scari, A. da-S.; Pockszevnicki, B.C.; Landre Junior, J.; Magalhaes Junior, P.A.A. (2014). Stress-strain compression of AA6082-T6 aluminum alloy at room temperature. *J. Struct.*, **2014**, 1-8. DOI:10.1155/2014/387680

Shekha, Y.A.; Mohammedamin, J.K. (2024). Assessment of heavy metal contamination in dust samples from industrial and non-industrial sites in Erbil governorate. *Raf. J. Sci.*, **33**(3E).

DOI:10.33899/rjs.2024.184537
Strauss, G.N.; Pulker, H.K.; Ionenphysik, I.; Dünnschichttechnologie, A.G. (2005). Publikationen 2005-7 mechanical stress in optical coatings. *PhysT. Coat. Tech. GmbH*, 1-16. DOI:api.semanticscholar.org/CorpusID:53338500
Villalta-Cerdas, A.; McCleary, C. (2019). Analysis of copper alloys as an introduction to data analysis and interpretation for general chemistry courses. *Edu. Quím*., **30**(2), 41-53. DOI:10.22201/fq.18708404e.2019.2.67346
Wang, H.; Jiang, B.; Yi, D.; Wang, B.; Liu, H.; Wu, C.; Shen, F. (2019). Microstructure, corrosion behavior and mechanical properties of a non-isothermal ageing treated cast Al-4.5Cu-3.5Zn-0.5Mg alloy. *Mat. Res. Exp*., **7**(1), 16547. DOI:10.1088/2053-1591/ab638a
Yan, N.; Hong, Z.Y.; Geng, D.L.; Wang, W.L.; Wei, B. (2012). Phase separation and structure evolution of ternary Al-Cu-Sn immiscible alloy under ultrasonic levitation condition. *J. All. Com*., **544**, 6-12. DOI:10.1016/j.jallcom.2012.07.147
Zhang, S-Ch; Pan, Q.-I; Yan, J.; Huang, X. (2016). Effects of sliding velocity and normal load on tribological behavior of aged Al-Sn-Cu alloy. *Trans. Nonfer. Metals Soc. China*, **26**(7), 1809-19. DOI:10.1016/S1003-6326(16)64292-9

دراسة شاملة للسبائك الثلاثية من الالمنيوم والنحاس والقصدير والالمنيوم والنحاس والزنك مع اختبار الضغط والتأكسد

رائق رافع عمر النعمة **محمود أحمد حمود الجبوري**

قسم الفيزياء/ كلية العلوم/ جامعة الموصل/ العراق

الملخص

تعتبر السبائك الثلاثية المصبوبة محل دراسة كبيرة. على سبيل المثال، الألومنيوم (Al)، والنحاس (Cu)، والقصدير (Sn)، التي تصنع السبيكة الثلاثية لـ Al-Cu-Sn. مثال آخر، الألومنيوم (Al)، والنحاس (Cu)، والزنك (Zn)، التي تصنع السبيكة الثلاثية لـ Al-Cu-Zn. كل من هذه السبائك البديلة تتركز هنا في هذه الدراسة. يتم إنشاء كل واحد منهم تحت ظروف درجات حرارة عالية جدًا. يتم جمع عناصرها وضبط الأوزان وتقطيعها. لذلك، يتم تصنيع سبائك الصب الثلاثية. ثم يتم إجراء ومقارنة الاختبارات الميكانيكية الهامة للضغط والتآكل. تم إجراء اختبار الضغط لكل سبيكة من Al-Cu-Sn وAl-Cu-Zn. يمكن أن نستنتج أن أعلى قيمة ضغط يتم قياسها على أنها Zn=0% وSn=0%، ولكن يتم قياس أدنى قيمة ضغط على أنها Zn=10% وSn=10%. ومن ناحية أخرى، وجد أن تأثير اختبارات التآكل على كلا السبيكتين غير معنوي. النتائج الرئيسية لنتائج الضغط، والتي ترتبط بتركيزات Zn/Sn، هي أنه عندما يكون Zn=0% وSn=0%، تكون حالة السبيكة هشة، بينما عندما يكون Zn=10% وSn=10%، تكون حالة السبيكة مطيلة.

الكلمات الدالة: السبائك الثلاثية، اختبار الضغط، اختبار التآكل.